



Slovak Society of Chemical Engineering
Institute of Chemical and Environmental Engineering
Slovak University of Technology in Bratislava

PROCEEDINGS

48th International Conference of the Slovak Society of Chemical Engineering SSCHE 2022 and
Membrane Conference PERMEA 2022

hotel SOREA HUTNIK I
Tatranské Matliare, High Tatras, Slovakia
May 23 - 26, 2022

Editors: Assoc. Prof. Mário Mihaľ - Published by the Faculty of Chemical and Food Technology
STU in Bratislava for the Institute of Chemical and Environmental Engineering in 2022

ISBN: 978-80-8208-070-7, EAN: 9788082080707

Matejčíková, A., Krošláková, S., **Štefaňák, J., Rajniak, P.**: Experimental investigation of inhomogeneities of primary drying during lyophilization: Impact of vials packing density, Editors: Mihaľ, M., In *48th International Conference of the Slovak Society of Chemical Engineering SSCHE 2022 and Membrane Conference PERMEA 2022*, Tatranské Matliare, Slovakia, 2022.

Experimental investigation of inhomogeneities of primary drying during lyophilization: Impact of vials packing density

Anna Matejčíková¹, Simona Krošláková¹, Ján Štefaňák², Eduard Tichý³, Pavol Rajniak¹

¹Department of Chemical and Biochemical Engineering, Institute of Chemical and Environmental Engineering, Faculty of Chemical and Food Technology, Slovak University of Technology in Bratislava, Radlinského 9, 812 37 Bratislava, Slovakia

² Sitno Pharma, Ltd., Bratislava, Slovakia

³hameln rds a.s., Modra

Key words: lyophilization, inhomogeneity, packing density

The aim of this work is to identify different drying rates depending on the vial position during lyophilization. This phenomenon is called edge vial effect. The edge vial effect results in different product quality throughout the batch, with corner vials tending to dry faster compared to centre vials. It is known that higher sublimation rates are caused by radiation. However the higher sublimation rates in the edge vials are present at shelf temperature higher than room temperature. Packing density was identified as another source of heterogeneity. Packing density depends on the number of competing vials (i.e. vials surrounding a monitored vial). Edge vials have lower packing density compared to central vials and therefore, sublimation is higher. In this study, the effects of packing density and radiation were quantified in relation to the vials position. Also, experiments were performed at different temperatures for identification the impact of radiation and conduction from the lyophilizer.

SP

Cond - 0



Experimental investigation of inhomogeneities of primary drying during lyophilization: Impact of the vials packing density

Anna Matejčíková^a, Eduard Tichý^b, Pavol Rajniak^{a,c,*}

^a Department of Chemical and Biochemical Engineering, Institute of Chemical and Environmental Engineering, Faculty of Chemical and Food Technology, Slovak University of Technology in Bratislava, Radlinského 9, 812 37, Bratislava, Slovakia

^b Hameln Co., Research, Development & Supply, Horná 1408/36, 900 01, Modra, Slovakia

^c Sitno Pharma Ltd., Rybné námestie 1, 81102, Bratislava, Slovakia

ARTICLE INFO

Keywords:

Lyophilization
Experimental
Packing density
Edge vial effect
Sublimation study

ABSTRACT

Inhomogeneous lyophilization (different drying rates at different locations of the lyophilizer), usually called edge-vial-effect, is a known but still not fully understood problem in freeze drying. The edge-vial-effect is a phenomenon in which vials positioned at the shelf edges and corners tend to dry more quickly compared to central vials. For example, in a recent study of Assegehegn et al. (2020) the authors observed that for all combinations of shelf temperature and chamber pressure studied, the highest product temperature, sublimation rate, and overall vial heat transfer coefficient are observed in front edge vials, whereas the lowest values are observed in center vials. This observation is usually explained by an additional heating from the chamber walls. However, the higher sublimation rates in the edge vials exist also at shelf temperatures higher than room temperatures, when one would expect cooling from the walls and subsequently lower sublimation rates in the edge vials. Another, less known source of inhomogeneous drying is the impact of the packing density of vials on the shelves that was identified by Placek et al. (1999). The key idea is that with increasing number of competitive vials (i.e. the vials surrounding a monitored vial) the amount of heat coming from the shelf and available for sublimation in the monitored vial is decreasing. In other words, a smaller packing density of vials leads to a faster drying. Carefully designed sublimation experiments with different patterns and combinations of active vials (filled with water and open for sublimation) and inactive vials (empty vials without stopper) proved significant impact of the packing density and its contribution to the total sublimation rate. Quantification of the experiments at the different shelf temperatures shows that the total sublimation rate in both, corner vials and central vials, increases with temperature. Also, the contribution of the packing density to the total sublimation rate increases with the shelf temperature. On the other hand, the impact of radiation and conduction from the lyophilizer walls and door decreases with increasing temperature until it starts to show the opposite trend. For the shelf temperature of 25 °C (i.e. higher than the ambient room temperature of 20 °C), the edge vials are cooled from the walls and therefore, the contribution of radiation for drying temperature of 25 °C is negative. It is expected that combination of the radiation cage (Ehlers et al., 2021) and specifically designed experiments employing inactive vials in the central part of the shelves can significantly reduce (or almost eliminate) inhomogeneous drying rates during lyophilization.

1. Introduction

Freeze drying (or lyophilization) is a standard method used for the preservation of perishable products such as labile injectable drugs (vaccines, therapeutic proteins, and others) without damaging them. The advantage of this method is not only increasing product stability due

to inhibition of chemical and physical degradation reaction, but also easy storage and transport [1].

Freeze drying process includes three main steps: (i) freezing step, (ii) primary drying, and (iii) secondary drying. Freezing step is an initial stage during which almost all solvent (up to 95%) is transformed into solid. Solvent is separated from solute, while solute became more concentrated. This concentrated solute is called "freeze concentrate"

* Corresponding author. Department of Chemical and Biochemical Engineering, Institute of Chemical and Environmental Engineering, Faculty of Chemical and Food Technology, Slovak University of Technology in Bratislava, Radlinského 9, Bratislava, 812 37, Slovakia.

E-mail address: pavol.rajniak@stuba.sk (P. Rajniak).

<https://doi.org/10.1016/j.jddst.2022.103550>

Received 9 March 2022; Received in revised form 6 June 2022; Accepted 26 June 2022

Available online 9 July 2022

1773-2247/© 2022 Elsevier B.V. All rights reserved.

Nomenclature

$A_{all\ vials}$	surface occupied by vials [m ²]	T_g'	glass transition temperature [°C]
$A_{competitive\ vials}$	surface occupied by competitive vials [m ²]	T_{max}	maximum allowable temperature [°C]
$A_{monitored\ area}$	surface of the monitored area [m ²]	T_p	product temperature [°C]
D	external diameter of a single vial [m]	t_{pd}	primary drying temperature [°C]
K_g	heat transfer coefficient by conduction [W.m ⁻² .K ⁻¹]	T_s	shelf temperature
K_c	heat transfer coefficient by direct contact [W.m ⁻² .K ⁻¹]	WFI	water for injection [–]
K_r	heat transfer coefficient by radiation [W.m ⁻² .K ⁻¹]	Δm	mass loss [g]
L	circle diameter [m]	Δm_{center}	amount of sublimed water in central vials [g]
m	mass weight [g]	Δm_{corner}	amount of sublimed water in corner vials [g]
P	pressure [mbar]	$\Delta m_{packing\ density}$	amount of sublimed due to the lower value of packing density at the corner vials [g]
P_{ch}	chamber pressure [mbar]	$\Delta m_{radiation/conduction}$	contribution of the water amount sublimed due to the heat transfer by radiation and conduction from the dryer walls and the guard rail [g]
T_c	collapse temperature [°C]	ϕ	Packing density [–]
T_{eu}	eutectic temperature [°C]		
TF	target fill [–]		

and contains only 20% of water (w/w) [2]. The second stage is primary drying. Primary drying is run at low pressure to promote sublimation of frozen water. During this stage, all frozen water is removed, but samples still contain a fair amount of unfrozen water (5–20%), depending on the formulation. Residual moisture is removed during the secondary drying by desorption. Secondary drying is run at a temperature higher than the temperature used for primary drying. Residual moisture is reduced to an optimal level, usually about 1–3% [3]. The quality of the final products depends on the process conditions of all these steps. Indeed, different process conditions affect the performance of individual stages and also the quality of the final product is influenced. Every stage is also a possible source of heterogeneity. Differences in ice nucleation temperature during freezing may be a source of heterogeneity during drying, as different nucleation temperatures result in different resistance to water vapor mass transfer and therefore different behavior during primary drying (higher temperatures/longer drying times in vials that nucleate at the lowest temperature). These heterogeneities lead to variation in the quality of intra- and inter-batch. Understanding the source of heterogeneity is important for successful freeze drying. This study is focused on the identification and quantification of heterogeneity sources during primary drying.

2. Theory of primary drying inhomogeneities

During primary drying, the majority of water is removed from the frozen solution by sublimation obtaining a porous structure. During this step, product temperature (T_p) must be kept below the maximum allowable temperature (T_{max}). If product temperature is higher than a critical value, frozen material undergoes a viscous flow, which is known as collapse [4]. The maximum allowable temperature is usually 2–3 °C below the collapse temperature (T_c) and depends on the formulation. For amorphous formulation, T_{max} is associated with glass transition temperature (T_g') and, for crystalline formulation, T_{max} is associated with eutectic temperature (T_{eu}). However, product temperature is not controlled directly and varies through the batch. Usually, vials located at the periphery have a higher product temperature than central vials and therefore, products in periphery vials are prone to collapse. Product temperature is handled by setting a chamber pressure (P_{ch}) and shelf temperature (T_s). Therefore, balancing between heat input to the product and heat removal from the product by sublimation is crucial for successful lyophilization, and heterogeneities between central and periphery vials must be considered [5].

2.1. Heat transfer in lyophilization

Heat transfer is heat exchange between vials and shelf on which vials

are loaded, heat transfer from walls and door, and also, from the shelf above the vials. Based on these, heat transfer coefficient is a sum of three main mechanisms: (i) heat transfer by gas conduction between the shelf and the bottom of vials (K_g), (ii) heat transfer by conduction from shelf to vial at points of direct contact (K_c), and (iii) heat transfer by radiation (K_r) [6]. All three mechanisms are important, but the relative importance of these contributions depends on the type and geometry of vials, chamber pressure, and vials configuration. Thermal radiation is not a dominant mechanism because of low temperature, but radiation became an issue when relatively warm surfaces are present, e.g. door and chamber walls. Rambhatla and Pikal confirmed the responsibility of atypical radiation for the position dependence of heat transfer through the batch. This effect is known as *edge vial effect* [7]. Vials located at the periphery (at front, back and sides of array), receive more heat during primary drying leading to a higher sublimation rate compared to the central vials. Also, edge vials are in direct contact with a metal guard rail, which transmits some heat from the shelf to the vials. The effect of guard rail on sublimation rate was studied by replacing the stainless steel with Styrofoam. Styrofoam decreased the sublimation rate at periphery vials, but the sublimation rate was still higher compared to the rate of sublimation in central vials. Therefore, the guard rail and radiation are not the only reasons for the higher sublimation rates [8]. In terms of heat transfer, stainless steel guard rail represents a radiation shield but also increases heat transfer by conduction. However, the net effect of heat transfer is decreased [7]. On the other hand, central vials are not affected by radiation. In the hexagonal arrangement, each central vial is surrounded by six vials. These adjacent vials provide a radiation shield and therefore, radiation is not a significant mechanism of heat transfer for central vials [9]. Very recently [10] published a detailed study of the impact of chamber wall temperature on energy transfer during freeze-drying. They tried to minimize the radiation coming from the chamber wall during lyophilization by installing a radiation cage inside the lyophilizer and by setting it at different low temperatures to determine the impact of chamber wall temperatures below 0 °C on product temperature. Corner and center vials ran more homogeneous with radiation cage since the edge and corner vials were slowed down. The difference in primary drying time between corner and center vials in the tray could be significantly reduced (7 h) when the radiation cage was controlled at product temperature and combined with a higher shelf temperature. They concluded that the radiation cage is a useful tool for a more homogeneous batch with the potential to reduce primary drying time. Nevertheless, the drying difference between corner and center vials could only be reduced and was not completely eliminated. It is very complex – and probably still impossible – to develop and validate a completely ‘a priori’ model able to predict heat transfer differences and edge vial effects. Gravimetric studies

[11–13] provide data for subsequent simple, cheap and straightforward calculation of apparent Heat Transfer Coefficients (HTCs) at selected vials on the shelf and subsequent using of the HTCs in mathematical models [13].

2.2. Packing density

Radiation and the presence of guard rail are not only reasons of heterogeneities during primary drying. Another possible cause of heterogeneity is packing density, originally proposed by Placek [8]:

$$\phi = \frac{\text{shelf surface occupied by vials within a distance } L}{\pi L^2} \quad (1)$$

Where L was chosen as $L = 3D$. The aim of the packing density definition is to quantify the impact of adjacent vials on the sublimation rate during primary drying. The key assumptions are that active surrounding vials are competitors for the heat received from the shelf and the surface area of the bottoms of surrounding vials is relevant for the heat exchange between the shelf and the surrounding vials.

Generally, packing density depends on two factors and thus, (a) the position of the vial and (b) vials arrangement. As regards a vial position, periphery vials are termed as atypical vials because they are not surrounded by six neighbor vials as central vials. They receive more heat and therefore, sublimation rate is higher at edge vial. The presence of neighbor vials reduces the heat transfer to the vial resulting in a lower sublimation rate in central vials (Gieseler and Lee, 2008). In addition to a vial position, also vials arrangement influences the vials packing density. There are two main arrangements of vials: hexagonal array usually used in practice and square array of vials. Hexagonal packing is preferred over square packing due to higher productivity. Vials arranged in a hexagonal array can be divided into five groups based on their position: (i) corner vials, (ii) outer edge, (iii) inner edge, (iv) front and back row, (v) and central vials, as shown in Fig. 1. Vials in each group have a different number of neighbor vials which are considered as competitive vials in heat transfer. Vials in these categories receive different heat flux leading to different sublimation rates [14]. The greatest differences are between corner vials and central vials. While corner vials have only two adjacent vials, central vials have up to six adjacent vials.

The second, but less frequently used vials arrangement is square

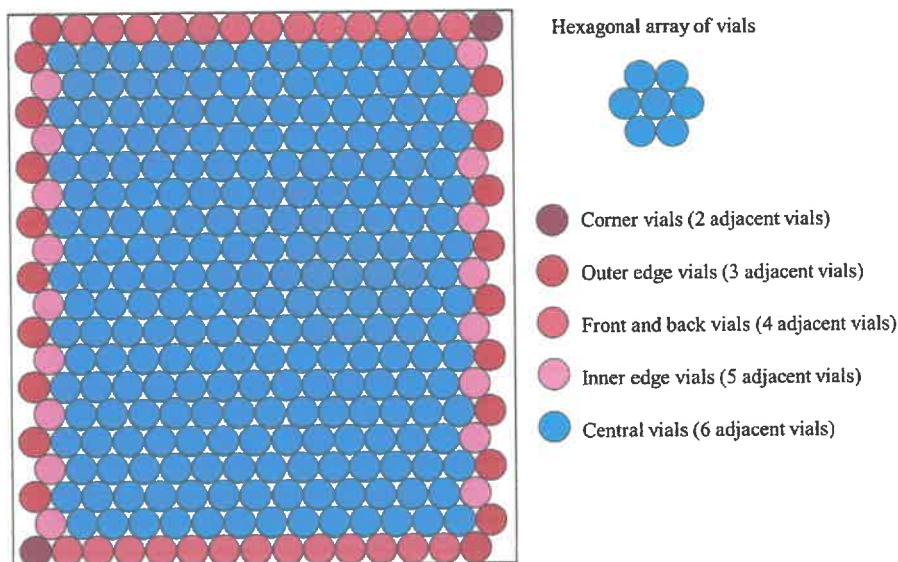


Fig. 1. Classification of vials into five categories according to their position: corner vial, front/back row, inner edge vial (without contact with stainless steel rail), and outer edge vial (contact with stainless steel guard rail) and central vials. The classification facilitates the definition of sources of heterogeneity during primary drying.

packing (Fig. 2). A disadvantage of this packing is a lower loading capacity compared to the hexagonal array of vials. For square packing, vials are divided into four groups: (i) corner vials, (ii) edge vials, (iii) front and back vials, and (iv) central vials. Regarding the number of adjacent vials, there are only three different groups (corner, periphery, and central vials) that receive different heat fluxes [15].

The differences between central and corner vials in hexagonal and square packing can be reduced by vials nested in a rack system. Vials in the rack system are separated by a certain distance from each other, so there are not competing vials present. Lyophilization in a rack system allows more homogeneous drying, and thus, the edge vials effect is decreased. The differences in product temperature T_p between corner and central vials were reduced from 39% to 27% [16]. The impact of the rack system was also confirmed in another study [17]. The separation of the vials in a plastic rack system ensured the same packing density for corner vials and central vials, which then lead to almost the same

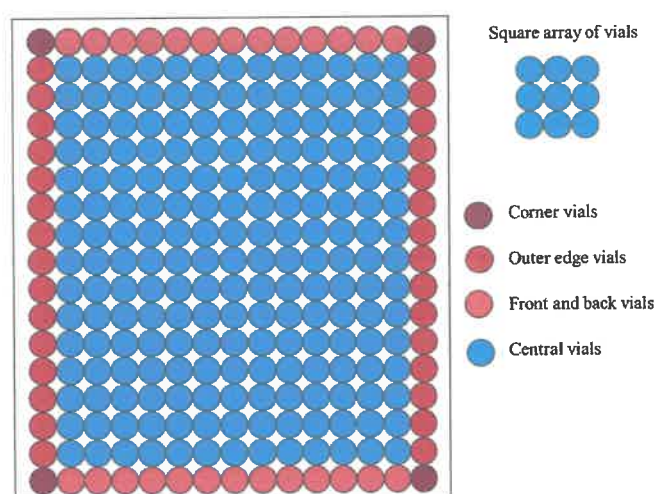


Fig. 2. Classification of vials into four categories according to their position: corner vial, front/back row and outer edge vials (contact with stainless steel rail) and central vials. The classification facilitates the definition of sources of heterogeneity during primary drying.

(homogeneous) rate of sublimation [17].

Vial packing density appears to be an important source of inhomogeneity, while the arrangement of the vials as well as the position of the vial must be considered. This study is focused on the quantification of individual sources of inhomogeneities and the determination of the effect of packing density is one of them.

3. Materials and methods

3.1. Materials

The experiments were carried out with vials of the 10R type. The 10 ml injection vials (10R) are manufactured out of tubular clear borosilicate glass of the 1st hydrolytic class. The dimensions are ϕ 24.0 x 45 x 1.00 mm. The vials were filled with water for injection (WFI). Target fill (TF) was the same for all vials in all experiments, i.e. TF = 5 ml. Vials were semi-closed with 20 mm rubber freeze drying injection stoppers, grey, suitable for 20 mm crimp neck vials, which have openings for vapor flow.

3.2. Freeze-dryer

Freeze dryer Martin Christ Epsilon 2-10D LSC was used. The dryer has the ice condenser capacity of 10 kg, 5 shelves with the temperature controlled in the range -55 °C to $+60$ °C and the total shelf area of 0.98 m². The dryer is equally ideal for product development and small-scale production activities.

3.3. Freeze drying procedure

The experiments were performed under conditions which cover relatively broad range of temperature and pressure typically used for lyophilization cycle. Only a single shelf (the middle one) was loaded in all experiments, always with 300 vials which were sequentially numbered, filled with water for injection, and placed directly on the shelf with hexagonal packing arrangements surrounded by a metal guard rail. Experiments at the chamber pressure 0.25 mbar and different shelf temperature are summarized in Table 1 and were used for the analysis in this paper.

An example of the freeze-drying cycle for sublimation studies is showed in Table 2. The duration of each step is the same for each experiment. A fast decrease of the chamber pressure from the atmospheric pressure to 0.25 mbar and the shelf temperature ramp rate of 0.667 °C/min were employed at the start of sublimation.

3.4. Gravimetric evaluation of the mass sublimed

Mass sublimed was evaluated by weighing all active vials filled with water before (m_1) and after (m_2) the sublimation test. A high precision (0.00001 g) Mettler Toledo XPE 105 laboratory balance was used for the gravimetric measurements. As shown in Table 2, samples are frozen to -45 °C followed by sublimation at -15 °C for 190 min. The total mass loss in a vial (Δm) is calculated according to equation (2):

$$\Delta m = m_1 - m_2 \quad (2)$$

Table 1

A summary of experimental conditions during sublimation tests.

	$T_s = -25$ °C	$T_s = -15$ °C	$T_s = -5$ °C	$T_s = +5$ °C	$T_s = +25$ °C
$P_{ch} = 0.25$ mbar	X	X	X	X	X

Table 2

An example of freeze-drying cycle at shelf temperature = -15 °C and chamber pressure = 0.25 mbar.

Step	Time	Shelf temperature [°C]	Pressure [mbar]	
	Duration [min]			Total [hh:mm]
Loading	0	00:00	5	–
Freezing	270	04:30	-45	–
Freezing	60	05:30	-45	–
Sublimation	30	06:00	-45	0.25
Sublimation	45	06:45	-15	0.25
Sublimation	145	09:10	-15	0.25

3.5. Calculation of packing density

The vial packing density was originally proposed by Placek (2001) and later also by Gieseler (2007) as a fraction of the shelf surface occupied by vials within a distance L ,

$$\phi = \frac{A_{all\ vials}}{A_{monitored\ area}} \quad (3)$$

where ϕ is packing density, $A_{monitored\ area} = \pi L^2$ and $A_{all\ vials}$ is the surface area occupied by all vials located in the $A_{monitored\ area}$. In this study we propose a modified definition of the packing density as a ratio of the area occupied by competitive vials located in monitored area and total monitored area:

$$\Phi = \frac{A_{competitive\ vials}}{A_{monitored\ area}} \quad (4)$$

So the main difference is, that the $A_{competitive\ vials} = A_{all\ vials} - A_{monitored\ vial}$. The new definition means, that for a single vial which has all neighboring vials inactive (for example fully stoppered) is the packing density $\Phi = 0$.

For the analysis presented in this work we decided to define the monitored area as a circle with a diameter $L = 2D$, where D is the external diameter of a single vial. Examples of the packing density defined by equation (4) are presented in Fig. 3 for corner vial (vial number 1) and central vial (vial number 33). The light green colored vials represent monitored vials for which packing density is calculated (Φ_1 and Φ_{33}). The monitored area is bounded by a red circle with a

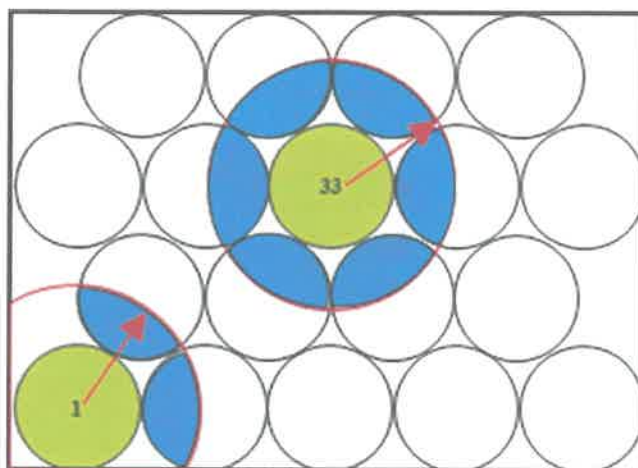


Fig. 3. Example of packing density evaluation for vial number 1 (corner vial) and vial number 33 (central vial). A red circle bounds the monitored area. Green areas illustrate vials for which the packing density is calculated. Blue vial sections represent the area of competing vials located in the monitored area. (For interpretation of the references to color in this figure legend, the reader is referred to the Web version of this article.)

diameter $L = 2D$, i.e., $L = 4.4$ cm for the 10R vials. The blue sections represent area of the neighboring (competitive) vials in the monitored area.

For the vial number 1 (corner vial), only two neighboring vials (blue sections) compete with the vial 1 in the monitored area, while for the vial 33 (central vial) 6 vials (blue sections) compete with the vial 33 in the monitored area. To evaluate the packing density, the area of the blue segments had to be calculated. The AutoCAD® software has been used for the calculation of the area of the blue sections.

The packing density varies with respect to the vial position. Vials at different shelf locations have different number of neighboring (competing) vials. To evaluate the impact of packing density on mass sublimed, the vial packing density is evaluated for all vials on the shelf.

3.6. Quantification and separation of the effects of radiation and packing density

The sublimation rate depends on the vial position on the shelf. The biggest difference is between periphery and central vials, with the sublimation rates higher at periphery. Periphery vials are surrounded by a smaller number of competing vials and also, they are exposed to the heat radiation and conduction from the dryer walls. Both, the radiation/conduction from the walls and the guard rail and the packing density contribution impact the drying rate. The value of packing density is maximal for central vials and the heat transfer by radiation/conduction is minimal for the central vials. Based on these assumptions, the total amount of water sublimed from the corner vial Δm_{corner} is a summation of following contributions:

$$\Delta m_{corner} = \Delta m_{center} + \Delta m_{packing\ density} + \Delta m_{radiation/conduction} \quad (5)$$

Δm_{center} is the amount of sublimed water in central vials at a maximum value of packing density [g],

$\Delta m_{packing\ density}$ is the contribution of the water amount sublimed due to the lower value of packing density at the corner vials [g],

$\Delta m_{radiation/conduction}$ is the contribution of the water amount sublimed due to the heat transfer by radiation and conduction from the dryer walls and the guard rail [g].

To test and quantify equation (5) we have designed and performed different experiments, in which we investigated impact of decreasing packing density on the sublimation rate. The positioning and distribution of active vials (blue, filled with water and opened) vs. inactive vials (white, filled with water and fully stoppered) is illustrated in Fig. 4.

Fig. 4a shows a packing pattern created by four rows of inactive vials and 2 vials surrounded (isolated) by a single circle or by two circles of inactive vials. Fig. 4b depicts three isolated vials, each surrounded by different number of inactive vials. The isolated central vials do not have active neighbors which would compete for the heat from the shelf and consequently, their packing density is lower. Besides that, vials located in the middle of the shelf and the effect of radiation/conduction from walls and guard rail can be neglected, while the mass loss is impacted mainly (or only) by the lower packing density.

4. Results and discussion

4.1. Evaluation of packing density

The packing density is evaluated for each experiment. In the case of full packing (Fig. 1), packing density is in the range from 0.35 to 0.67. For different packing patterns, the individual packing density values were color-coded, while the packing density is in the range 0.0–0.67 as shown Fig. 5.

Fig. 5a shows packing pattern with white vials representing inactive vials. Vials located in the middle of the circles are active (marked in burgundy) and because they are surrounded by inactive vials, their packing density is 0. Regarding their position far from the walls and guard rails, the effect of radiation and conduction is negligible. Therefore, the amount of sublimed water is affected only by the value of packing density. Further, each inactive vial affects packing density of all neighbors with which is in direct contact. Thus, the value of packing density of active vials adjacent to the inactive vials is decreasing from vial packing density corresponding to turquoise (maximal value of packing density) to green and light green values. As a result, the packing density in specific central vials is similar to the packing density corresponding to the periphery vials.

Fig. 5b shows again an experiment with empty circles and empty rows. Even these empty rows of vials affected the value of packing

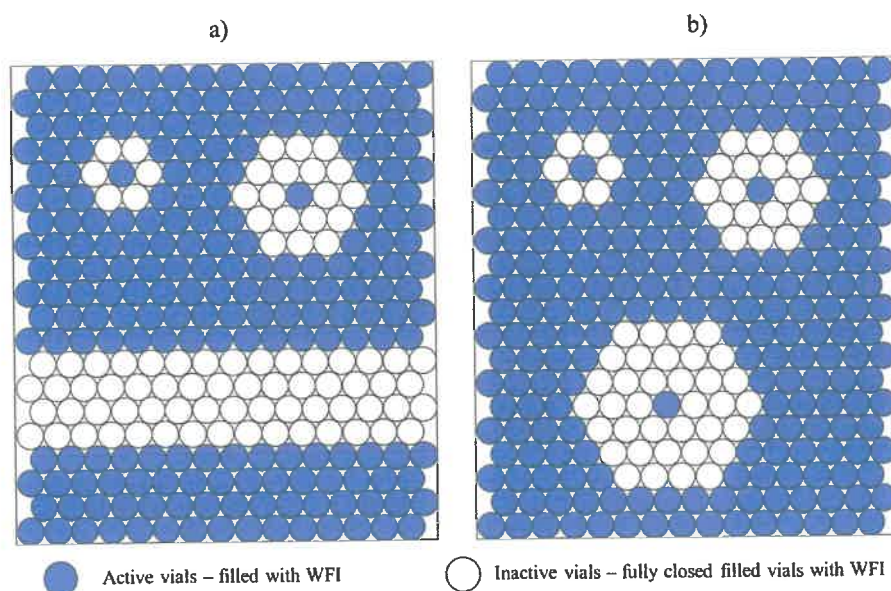


Fig. 4. Design of experiment to quantify the effect of packing density and the effect of radiation on sublimation rates. Blue vials are active vials, i.e., vials filled with water and opened for sublimation. White vials represent inactive vials, i.e. vials filled with water but fully closed by stoppers. (For interpretation of the references to color in this figure legend, the reader is referred to the Web version of this article.)

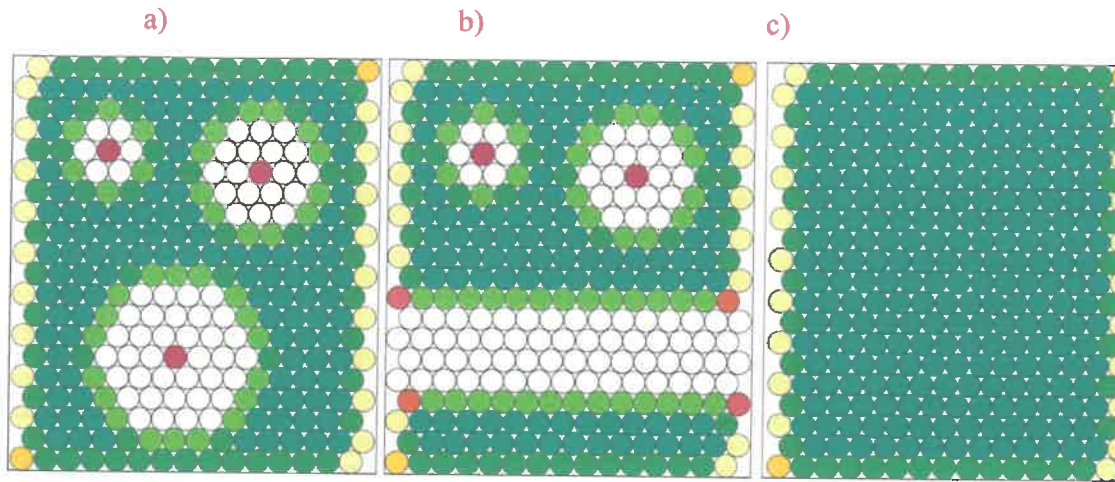


Fig. 5. Evaluation of packing density for different vial arrangements. Fig. 5 a) shows a packing with three active vials surrounded by one, two and three circles of inactive (white) vials. Fig. 5 b) displays also four rows of inactive vials surrounded by active vials. Fig. 5c) shows packing density of full packing. The legend illustrates by different colors the corresponding packing densities of the active vials. (For interpretation of the references to color in this figure legend, the reader is referred to the Web version of this article.)

density of the central vials. Vial packing density of central vials adjacent to inactive vials rows correspond to the packing density of vials in the front/back row. Finally, Fig. 5c illustrates packing densities of different vials of the full hexagonal packing.

4.2. Inhomogeneous primary drying

Heterogeneities are identified gravimetrically with respect to the vial positions on the shelf. The value of mass sublimed in each vial is marked by a color code. The following Fig. 6 shows inhomogeneity for standard full packing. The amount of mass sublimed at periphery vials is higher compared to the central vials. Sublimation at periphery is enhanced due to the effect of radiation and lower packing density. Also, the inhomogeneity ratio is evaluated as a ratio of the maximum and minimum amount of sublimed water. Inhomogeneity ratios are 2.57 and 2.26 for sublimation temperature $-25\text{ }^{\circ}\text{C}$ and $-15\text{ }^{\circ}\text{C}$, respectively.

Also, the dependence of the mass sublimed on the vial packing density is evaluated, while vial packing density is calculated for each active vial according to equation (1). The packing density for the vial number 1 is calculated as follows:

$$\Phi_1 = \frac{A_{\text{competitive vials}}}{A_{\text{monitored area}}} = 0.35 \tag{6}$$

Where Φ_1 is packing density for vial number 1.

$A_{\text{competitive vials}}$ is total area occupied by competitive vials in monitored area [m^2]
 $A_{\text{monitored}}$ is monitored area within the guard rail [m^2]

The average amounts of sublimed water depending on the packing density are shown in Fig. 7. Both dependences exhibit the same trend. The higher packing density, the lower mass sublimed. The lower packing density (0.35) corresponds to the corner vials, while the highest packing density (0.67) corresponds to the central vials.

Similarly, heterogeneities are identified for experiments with different patterns performed at sublimation temperatures $-5\text{ }^{\circ}\text{C}$, $+5\text{ }^{\circ}\text{C}$, and $+25\text{ }^{\circ}\text{C}$ and presented in Fig. 8. The amount of mass sublimed is marked by the same color coding. Also in this case, the sublimation rate is enhanced at the periphery compared to the central vials. But inactive vials also influence the amount of mass sublimed in adjacent vials. Mass sublimed in vials adjacent to empty rows (Fig. 8a) and b) is higher. Average mass sublimed is comparable with mass sublimed in vials located in the front row. This is caused by lowering packing density. Furthermore, central isolated vials located in inactive circles (Fig. 8a, b, and Fig. 8c) have even higher mass sublimed than vials adjacent to the empty rows. Those vials are central vials without the radiation impact, i.

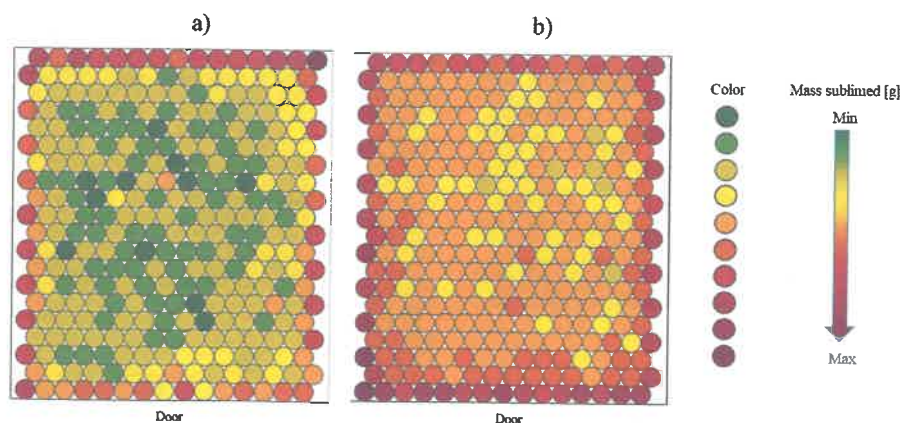


Fig. 6. Evaluation of inhomogeneities depending on the vial position. Fig. 6a shows heterogeneity at sublimation temperature of $-25\text{ }^{\circ}\text{C}$, and Fig. 6b shows heterogeneity at sublimation temperature of $-15\text{ }^{\circ}\text{C}$. Both experiments were performed at the chamber pressure 0.25 mbar.

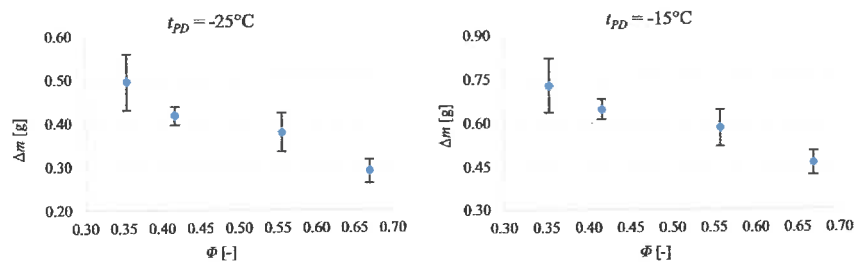


Fig. 7. The dependence of average amount of mass loss for different values of vials packing density at different sublimation temperature, i.e., at temperature -25°C and -15°C . For these experiments, full packing of active vials was used.

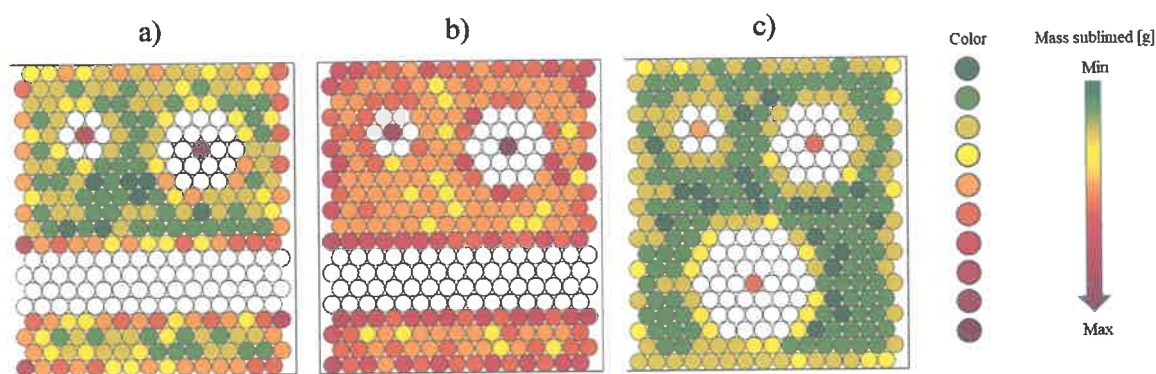


Fig. 8. Evaluation of inhomogeneities within the batch with different patterns created by inactive vials. Fig. 8a shows heterogeneity at sublimation temperature of -5°C , Fig. 8b illustrates heterogeneity at sublimation temperature $+5^{\circ}\text{C}$ and Fig. 8c shows heterogeneity at sublimation temperature $+25^{\circ}\text{C}$. All experiments were performed at the chamber pressure 0.25 mbar.

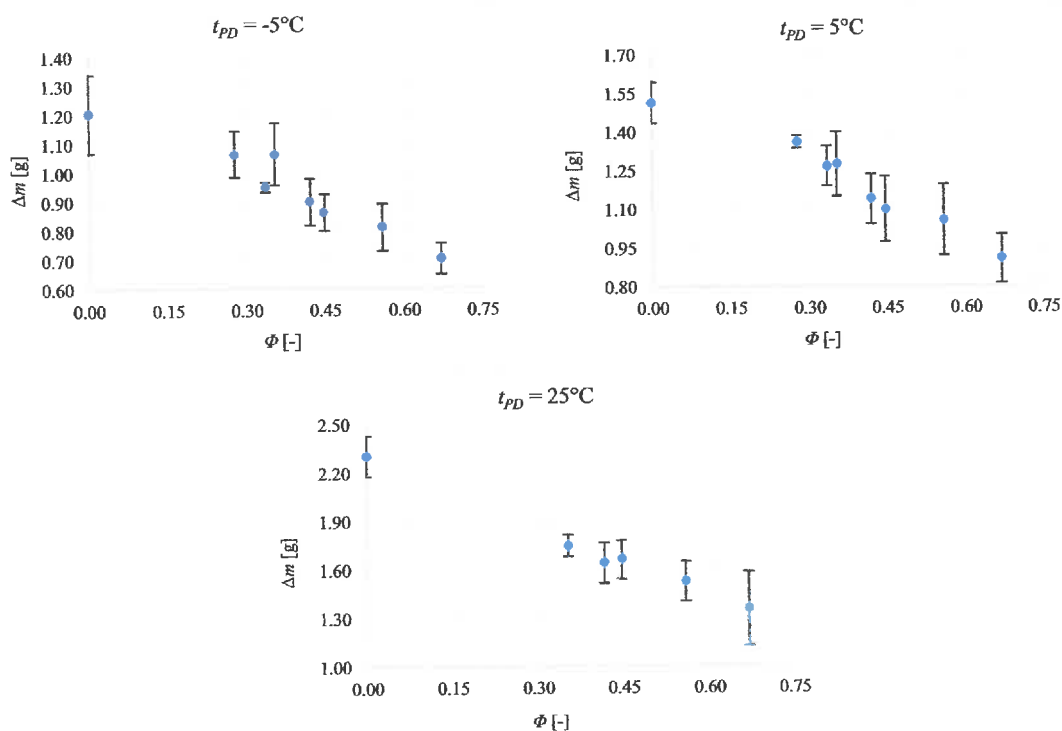


Fig. 9. The dependence of average amount of mass loss for different value of the vials packing density at different sublimation temperatures. For these experiments, different patterns created by inactive vials were used.

e., a higher amount of mass sublimed results from lower packing density. If the central vials do not have competitors (i.e., they are surrounded by inactive vials), they can be almost as "fast" as the edge vials, or even higher depending on sublimation temperature. Regarding the number of circles created by inactive vials, two inactive circles of vials lead to a higher amount of mass loss compared to the one inactive circle. However, three inactive circles of vials do not further increase the amount of sublimed water. Therefore we conclude that it is sufficient to use only two inactive circles for the quantification of the limiting packing density impact.

Fig. 9 shows the dependence of water sublimed on the value of packing density. Packing density for experiments with inactive vials patterns takes values in the range 0.00–0.67. Using inactive vials, packing density for central vials is reduced from the value 0.67 to values from 0.00 to 0.45. Packing density zero corresponds to isolated central vials. As can be seen in Fig. 9, the highest mass loss is for isolated vials with the lowest value of packing density. However, these vials are not affected by radiation and therefore, the amount of water sublimed is affected only by the packing density. Since the packing density is zero, the water sublimed in isolated vials is considered as the highest possible sublimed water for central vials under the given conditions.

4.3. Quantification of the packing density impact

Experiments with inactive vials were used for quantification and separation of the effects of radiation vs. packing density. The following

procedure was used for quantification:

1. Only experiments with not standard packing patterns were used to quantify the effect of packing density, while central vials have different values of packing density due to the inactive vials.
2. Then, central vials with a different value of packing density are selected, while vials have to be at least three rows away from the edge. The radiation/conduction from walls and guard rail has a negligible effect on these vials and therefore, only the packing density impacts the mass sublimed. For all experiments, vials located in the same position were selected.
3. Subsequently, the dependence of the amount of sublimed water on the packing density was evaluated and is illustrated in Fig. 10. The relationship between observed data was fitted by linear regression for each sublimation temperature.
4. According to linear regression and equation (4), the quantification of the effect of the packing density and the effect of radiation is evaluated for the corner vial number 1. The packing density for the corner vial 1 is 0.35. It must be noted, that for periphery vials only monitored area located within the guard rail is considered. Therefore, the monitored area for vial number 1 is not a circle with a diameter of 4.4 cm but only the corresponding section of this circle.

For the sublimation temperature of $-5\text{ }^{\circ}\text{C}$, the following linear equation describing the dependence between mass sublimed and packing density was evaluated:

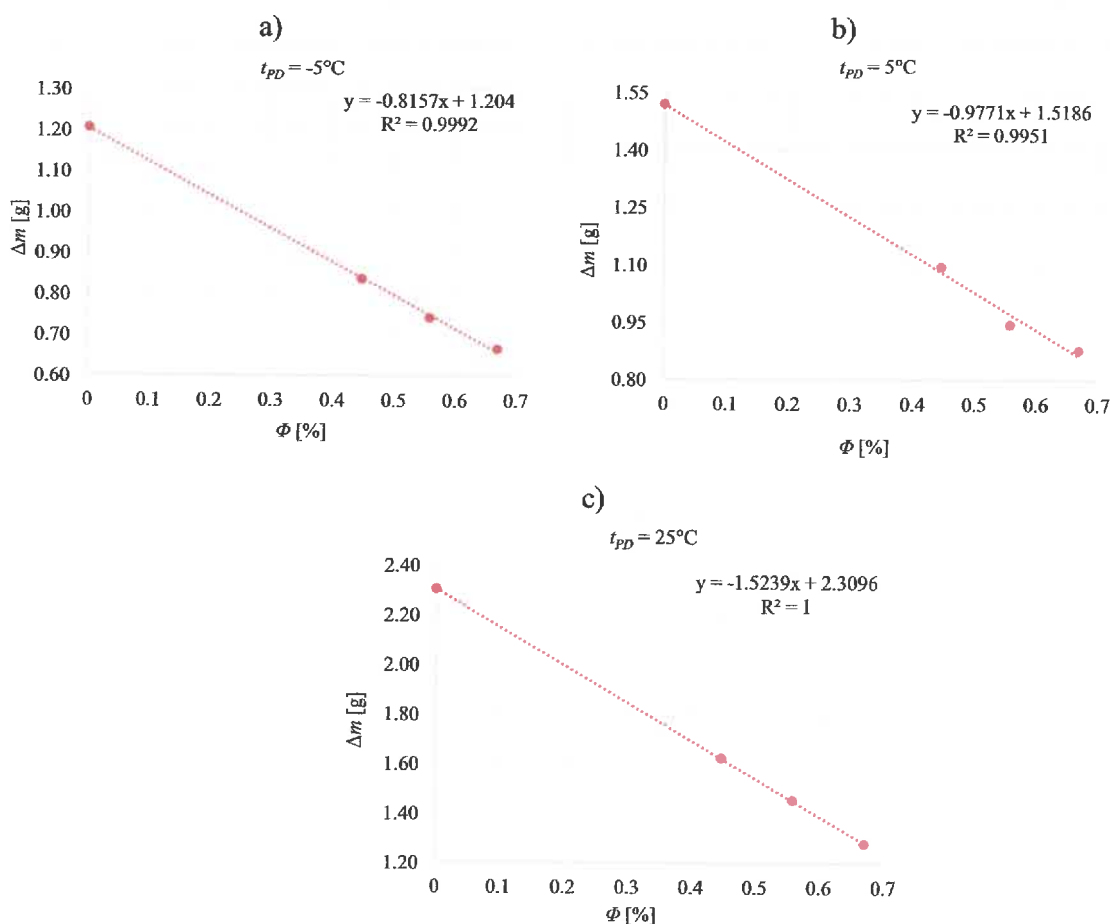


Fig. 10. The figure shows the dependence of the amount of sublimed water on the packing density for central vials at different sublimation temperature. Fig. 10a shows the dependence at the sublimation temperature of $-5\text{ }^{\circ}\text{C}$, Fig. 10b is for the sublimation temperature $5\text{ }^{\circ}\text{C}$ and Fig. 10c is for the sublimation temperature $25\text{ }^{\circ}\text{C}$.

$$\Delta m = -0.8157 \cdot \Phi + 1.204 \quad (7)$$

For corner vial, total mass loss is summation of three different contributions (Equation (5)) as follows: (i) $\Delta m_{\text{central vials}}$, (ii) $\Delta m_{\text{packing density}}$, and (iii) $\Delta m_{\text{radiation/conduction}}$. The first contribution, $\Delta m_{\text{central vials}}$, is an average mass sublimed in central vials with the highest value of packing density, meaning an average mass sublimed in vials surrounded by six adjacent vials. The contribution of the central vial is evaluated directly from experiment. For sublimation temperature of -5°C , the average mass loss in central vials is $\overline{\Delta m}_{\text{central vials}} = 0.67\text{g}$.

Before quantifying the contribution of the packing density, it is necessary to calculate the amount of sublimed water for vials with packing density corresponding to the packing density of corner vials. Packing density for corner vials is 0.35 and the mass sublimed is calculated from equation (7). Evaluated mass sublimed consists of two contributions, i.e. the contribution of the central vial, $\Delta m_{\text{central vials}}$ and the contribution of the vial packing density, $\Delta m_{\text{packing density}}$:

$$\begin{aligned} \Delta m_{\text{packing density+central vial}} &= -0.8157 \cdot \Phi + 1.204 = -0.8157 \cdot 0.35 + 1.204 \\ &= 0.92 \text{ g} \end{aligned} \quad (8)$$

Based on this result, the contribution of vial packing density ($\Delta m_{\text{packing density}}$) is quantified:

$$\Delta m_{\Phi} = m_{\text{packing density+central vials}} - \overline{\Delta m}_{\text{central vials}} = 0.92 - 0.67\text{g} = 0.25 \text{ g} \quad (9)$$

The last contribution is the radiation/conduction contribution, $\Delta m_{\text{radiation/conduction}}$. It was calculated as a difference between experimentally measured value for corner vials and calculated value including the effect of packing density:

$$\Delta m_{\text{radiation}} = \Delta m_{\text{corner vials}} - \overline{\Delta m}_{\text{central vials}} - \Delta m_{\text{packing density}} = 1.14\text{g} - 0.67\text{g} - 0.25\text{g} = 0.22\text{g} \quad (10)$$

The same assumptions were also employed for another sublimation experiment. The results are summarized in the following Table 3:

The impact of individual contributions is summarized in Table 3 as follows:

With the increasing shelf temperature, the amount of mass loss in corner vial, $\Delta m_{\text{corner vials}}$, increases. The same trend applies to the contribution of central vials $\Delta m_{\text{central vials}}$, and to the contribution of packing density $\Delta m_{\text{packing density}}$, where the amount of sublimed water increases with increasing sublimation temperature. On the contrary, the radiation effect, $\Delta m_{\text{radiation/conduction}}$, decreases with rising temperature until it starts to show the opposite trends. Radiation effect is highest at the lowest sublimation temperature. Therefore, the radiation has the highest effect at the lowest temperature due to the biggest differences between the ambient temperature (usually about 20°C) and the drying temperature. If the drying temperature (e.g., 25°C) is higher than the ambient temperature (20°C), the edge vials are cooled from the walls and therefore, the contribution of radiation for drying temperature 25°C is negative. Different contributions are also shown in the following

Table 3
Quantification of packing density and radiation impact for different sublimation experiments.

t_{PD} [$^\circ\text{C}$]	$\Delta m_{\text{corner vials}}$ [g]	$\overline{\Delta m}_{\text{central vials}}$ [g]	Δm_{Φ} [g]	$\Delta m_{\text{radiation/conduction}}$ [g]
-5	1.14	0.67	0.25	0.22
5	1.36	0.88	0.30	0.18
25	1.70	1.29	0.49	-0.08

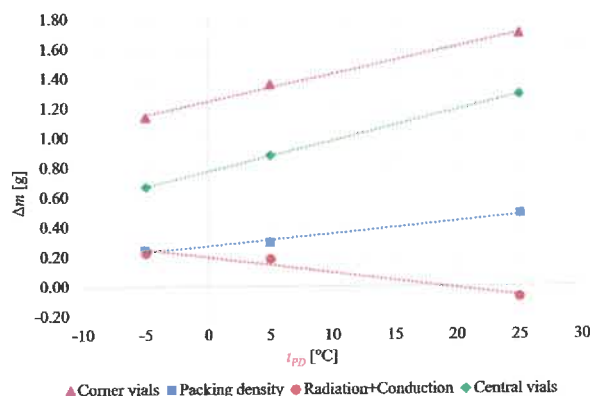


Fig. 11. Quantification of packing density and radiation impact.

Fig. 11.

It is also instructive to compare an inhomogeneity ratio (a ratio of $\Delta m_{\text{corner vials}}$ and $\overline{\Delta m}_{\text{central vials}}$ listed in Table 3. The inhomogeneity ratio at -5°C is 1.7 but it is only 1.3 at $+25^\circ\text{C}$. It further demonstrates decreasing impact of the radiation from walls but also shows that the drying difference between corner and center vials could only be reduced but not completely eliminated at these experimental conditions. This is a very similar observation and conclusion as in the recent work [10] focused on minimization of the impact of chamber wall by installing a radiation cage inside the lyophilizer. We believe that the above analysis helps to understand and quantify roles of different mechanisms to the

total sublimation rates at different locations on the shelf and at different process conditions. The experimental data can be also used for calculation of apparent heat transfer coefficients corresponding to those different mechanisms. A methodology and software for calculation of heat transfer coefficients were described in our recent publication [13].

5. Conclusion

Two main sources of heterogeneous sublimation (different drying rates) were experimentally identified and quantified. The first and well known is the impact of the heat radiation and conduction from the walls and door of the lyophilizer. The second (less known) source of inhomogeneous drying is the impact of the packing density of vials on the shelves. In this study, the packing density Φ is defined as a ratio of the area occupied by competitive vials located in a monitored area and the total monitored area:

$$\Phi = \frac{A_{\text{competitive vials}}}{A_{\text{monitored area}}}$$

The key idea is that with increasing number of competitive vials (i.e. the vials surrounding a monitored vial) the amount of heat coming from the shelf and available for sublimation in the monitored vial is decreasing. In other words, a smaller packing density of vials leads to a faster drying. Carefully designed experiments having different patterns and combinations of active vials (filled with water and open for sublimation) and inactive vials (empty vials without stoppers) proved significant impact of the packing density and its contribution to the total sublimation rate. Quantification of the gravimetric experiments at the same pressure and different shelf temperatures can be summarized and

concluded as follows:

1. Total sublimation rate in both, corner vials and central vials increases with temperature.
2. The impact of the packing density to the total sublimation rate also increases with the shelf temperature.
3. On the contrary, the impact of radiation and conduction from the lyophilizer walls and door decreases with rising temperature until it starts to show the opposite trend. For the shelf temperature of 25 °C (i.e. higher than the ambient room temperature of 20 °C), the edge vials are cooled from the walls and therefore, the contribution of radiation for drying temperature 25 °C is negative.

We believe that combination of the radiation cage [10] and specifically designed experiments employing inactive vials in the central part of the shelves can significantly reduce (or almost eliminate) inhomogeneous drying rates during lyophilization.

Declaration of competing interest

The authors declare the following financial interests/personal relationships which may be considered as potential competing interests:

Pavol Rajniak reports financial support was provided by Sitno Pharma Inc.

Acknowledgment

This publication was created with the support of the Operational Program Integrated Infrastructure for the project: Development of products by modification of natural substances and study of their multimodal effects on COVID-19, ITMS: 313011ATT2, co-financed by the European Regional Development Fund.

References

- [1] J.C. Kasper, G. Winter, W. Friess, Recent advances and further challenges in lyophilization, *Eur. J. Pharm. Biopharm.* 85 (2013) 162–169.
- [2] G. Assegehegn, E. Brito-de la Fuente, J.M. Franco, C. Gallegos, The importance of understanding the freezing step and its impact on freeze-drying process performance, *J. Pharmacol. Sci.* 108 (2018) 1378–1395.
- [3] X.Ch Tang, M.J. Pikal, Design of freeze-drying processes for pharmaceuticals: practical advice, *Pharmaceut. Res.* 21 (2004) 2.
- [4] M. Brulls, A. Rasmuson, Heat transfer in lyophilization, *Int. J. of Pharmaceutics* 246 (2002) 1–16.
- [5] S. Hübner, Ch Wagner, H. Gieseler, Vial freeze-drying, Part I: new insights into heat transfer characteristics of tubing and molded vials, *J. Pharmacol. Sci.* 101 (2012) 1189–1201.
- [6] M.J. Pikal, M.L. Roy, S. Shah, Mass and heat transfer in vial freeze-drying of pharmaceuticals: role of the Vial, *J. Pharmacol. Sci.* 73 (1984) 1224–1237.
- [7] S. Rambhatla, M.J. Pikal, Heat and Mass Transfer Scale-Up Issues during Freeze-Drying, I: Atypical Radiation and the Edge Vial Effect, 2003.
- [8] J. Placek, D.T. Kamei, G.K. Lee, S.J. Mosley, P. Rajniak, J.L. Zitomer, S.D. Reynolds, W.A. Hunke, Inhomogeneity Phenomena in Lyophilization, AAPS Congress, New Orleans, 1999.
- [9] M.J. Pikal, Heat and mass transfer in low pressure gases: applications to freeze drying, *Transp. proces. pharm. sys.* (2000) 611–686.
- [10] S. Ehlers, W. Friess, R. Schroeder, Impact of chamber wall temperature on energy transfer during freeze-drying, *Int. J. of Pharmaceutics* 592 (2021), 120025.
- [11] R. Pisano, D. Fissore, A.A. Barresi, P. Brayard, P. Chouvenec, B. Woinet, Quality by design: optimization of a freeze-drying cycle via design space in case of heterogeneous drying behavior and influence of the freezing protocol, *Pharmaceut. Dev. Technol.* 18 (2013) 280–295.
- [12] P.J. Van Bockstal, S.T.F.C. Mortier, J. Corver, I. Nopens, K.V. Gernaes, T. De Beer, Quantitative risk assessment via uncertainty analysis in combination with error propagation for the determination of the dynamic Design Space of the primary drying step during freeze-drying, *Eur. J. Pharm. Biopharm.* 121 (2017) 31–41.
- [13] P. Rajniak, J. Moreira, S. Tsinontides, D. Pham, S. Birmingham, Integrated use of mechanistic models and targeted experiments for development, scale-up and optimization of lyophilization cycles: a single vial approach for primary drying, *Dry. Technol.* 40 (2) (2022) 310–325.
- [14] K.H. Gan, O.K. Crosser, A.I. Liapis, R. Bruttini, Lyophilization in vials on trays: effects of tray side, *Dry. Technol.* 23 (2005) 341–363.
- [15] K.H. Gan, R. Bruttini, O.K. Crosser, A.I. Liapis, Heating policies during the primary and secondary drying stages of the lyophilization process in vials: effects of the arrangement of vials in clusters of square and hexagonal arrays on trays, *Dry. Technol.* 22 (2004) 1539–1575.
- [16] S. Daller, W. Friess, R. Schroeder, Energy transfer in vials nested in a rack system during lyophilization, *Pharmaceutics* 12 (2020) 61–71.
- [17] A. Matejčíková, P. Rajniak, Impact of packing density on primary drying rate, *Acta Chim. Slovaca* 13 (2020) 1–8.